J. KSIAM Vol.19, No.3, 289–303, 2015 http://dx.doi.org/10.12941/jksiam.2015.19.289

OPTIMAL IMPACT ANGLE CONSTRAINED GUIDANCE WITH THE SEEKER'S LOCK-ON CONDITION

BONG-GYUN PARK

PGM R&D LAB, LIG NEX1, SOUTH KOREA
E-mail address: bgpark0615@gmail.com

ABSTRACT. In this paper, an optimal guidance law with terminal angle constraint considering the seeker's lock-on condition, in which the target is located within the field-of-view (FOV) and detection range limits at the end of the midcourse phase, is proposed. The optimal solution is obtained by solving an optimal control problem minimizing the energy cost function weighted by a power of range-to-go subject to the terminal constraints, which can shape the guidance commands and the missile trajectories adjusting guidance gains of the weighting function. The proposed guidance law can be applied to both of the midcourse and terminal phases by setting the desired relative range and look angle to the final interception conditions. The performance of the proposed guidance law is analyzed through nonlinear simulations for various engagement conditions.

1. INTRODUCTION

In modern guidance law designs, impact angle control, which intercepts a target with specific direction, is required to maximize the warhead effect and the kill probability. However, since impact angle control makes the missile trajectories be highly curved and then may miss the target within the seeker's field-of-view (FOV), one should be careful to operate missiles with the seeker having a limited FOV when implementing the impact angle control. Also, since the seeker has the limited FOV and detection range, midcourse guidance should steer the missile toward the proper position where the seeker can successfully lock on the target when the target is located far away from the initial missile position.

Many researches on impact angle control have been conducted so far. Kim and Grider [1] presented a suboptimal guidance law for a reentry vehicle with impact attitude angle constraint, which is the first published paper relevant to impact angle control. Bryson and Ho [2] obtained an optimal solution for the rendezvous problem subject to the terminal position and velocity constraints, and the solution can be used for impact angle control by setting the rendezvous course to the collision one. Song et al. [3] proposed an optimal guidance law with impact angle constraint for varying velocity missiles against moving targets, and a target tracking filter is combined with the proposed guidance law for real implementation. Ryoo et al. [4] presented a generalized formulation of control energy minimization guidance laws with the desired impact

Received by the editors August 6 2015; Revised August 24 2015; Accepted in revised form August 24 2015; Published online September 24 2015.

angle for a constant speed missile with arbitrary order dynamics. As an extension of this work, they proposed an optimal guidance law with terminal angle constraint solving a linear quadratic optimal control problem with the control energy cost weighted by a power of time-to-go [5]. Ratnoo and Ghose [6] formulated an impact angle control problem as a nonlinear regulator problem and then solved the problem using state-dependent Riccati equation (SDRE) technique. Lee et al. [7] handled optimality of linear time-varying guidance laws with impact angle constraint using an inverse problem of optimal control theory.

Other approaches to deal with impact angle control problems utilize proportional navigation guidance (PNG). Kim et al. [8] proposed a biased PNG to intercept targets with angular constraint. This guidance law includes a supplementary time-varying bias term in conventional PNG in order to control the terminal angle constraint. Manchester and Savkin [9] introduced a circular-navigation-guidance (CNG) law, which is based on the principle of following a circular trajectory to the target, to achieve the desired impact angle. Ratnoo and Ghose proposed hybrid guidance laws to control the terminal angle constraint against stationary targets [10] and nonstationary nonmaneuvering targets [11]. The proposed guidance laws in [10, 11] produced an orientation trajectory for covering all impact angles from 0 to -π in the first phase and then PNG commands with $N \geq 2$ for stationary targets (or $N \geq 3$ for moving targets) to intercept the target with the desired impact angle in the final phase. Erer and Merttopçuoğlu [12] proposed another two phase-typed guidance law consisting of conventional PNG and biased PNG controlling the integral of bias to achieve the impact angle.

Most of the works mentioned above can apply to both of the midcourse and terminal phases, but do not guarantee the seeker's lock-on condition, in which the target is located within the FOV and detection range limits, at switching instant of guidance phases. Some works, which can consider the seeker's lock-on condition, have been carried out. Whang [13] proposed an optimal guidance law pointing a target at given range, which is obtained from linearized equations of motion. Also, Jeon and Lee [14] addressed a similar guidance problem with target pointing angle constraint at specific relative range, and they obtained the optimal solution by directly solving the nonlinear dynamic equations without any linearization. The works presented in [13, 14], however, have not considered the flight path angle constraint to control the missile velocity direction.

In this paper, an optimal guidance law with impact angle constraint considering the seeker's lock-on condition is proposed for a constant speed missile against a stationary target. First, a midcourse guidance law is derived based on optimal control theory, and then this guidance law is modified by changing the desired values at the end of the midcourse phase to the final interception values to be implemented in the terminal phase. Since the proposed guidance law minimizes the energy cost function weighted by a power of range-to-go, it can modulate the acceleration commands and the missile trajectories adjusting guidance gains of the weighting function.

The outline of the paper is as follows. The guidance problem is formulated in Section 2. Optimal guidance laws for the midcourse and terminal phases are derived in Section 3. Section 4 investigates the performance of the proposed guidance law through nonlinear simulations for various engagement conditions. Section 5 describes the conclusions of this work

2. PROBLEM FORMULATION

Consider the planar engagement geometry as shown in Fig. 1, where $X_I - O - Y_I$ is a Cartesian inertial reference frame. The subscripts 0 and d stand for the initial and desired states. V is the missile speed and a is the acceleration perpendicular to the velocity vector. r, γ, and λ are the relative range between the missile and the target, the flight path angle, and the line-of-sight (LOS) angle, respectively. Under the assumption that the angle of attack (AOA) is small, which means that small acceleration commands are generated, we can define the seeker's look angle σ as an angle between the missile velocity and LOS vectors.

The nonlinear equations of motion, expressed in a polar coordinate system, are

$$\dot{r} = -V\cos\sigma \tag{2.1}$$

$$\dot{\sigma} = \dot{\gamma} - \dot{\lambda} = \frac{a}{V} + \frac{V\sin\sigma}{r} \tag{2.2}$$

$$\dot{\gamma} = \frac{a}{V} \tag{2.3}$$

where the dot operator represents the derivative with respect to time t. The boundary conditions for the midcourse phase are given as

$$r(t_0) = r_0, \quad \sigma(t_0) = \sigma_0, \quad \gamma(t_0) = \gamma_0 \tag{2.4}$$

$$r(t_d) = r_d, \quad \sigma(t_d) = \sigma_d, \quad \gamma(t_d) = \gamma_d \tag{2.5}$$

Assuming that σ is small and dividing Eqs. (2.2) and (2.3) by Eq. (2.1), we have the following linearized state differential equations:

$$\begin{bmatrix} \frac{d\sigma}{dr} \\ \frac{d\gamma}{dr} \end{bmatrix} = \begin{bmatrix} -\frac{1}{r} & 0 \\ 0 & 0 \end{bmatrix} \begin{bmatrix} \sigma \\ \gamma \end{bmatrix} + \begin{bmatrix} -\frac{1}{V^2} \\ -\frac{1}{V^2} \end{bmatrix} a \tag{2.6}$$

Since the independent variable has changed from t to r, the boundary conditions of Eqs. (2.4) and (2.5) are expressed as

$$\sigma(r_0) = \sigma_0, \quad \gamma(r_0) = \gamma_0 \tag{2.7}$$

$$\sigma(r_d) = \sigma_d, \quad \gamma(r_d) = \gamma_d \tag{2.8}$$

The seeker's lock-on can be achieved when the relative range and the look angle with respect to the target are within the detection range and field-of-view (FOV) limits, respectively. Therefore, at the instant of the handover that switches from the midcourse phase to the terminal one, the lock-on condition can be defined as

$$r(t = t_s) \le r_{\text{seeker}}, \quad \sigma(t = t_s) \le FOV/2 \tag{2.9}$$

where t_s is switching time of guidance phases and r_{seeker} denotes the seeker's detection range.

3. OPTIMAL GUIDANCE LAW

In this section, optimal impact angle control guidance laws with the seeker's lock-on condition are derived minimizing the energy cost function weighted by a power of range-to-go subject to the terminal constraints. First, a midcourse guidance law is obtained using linear

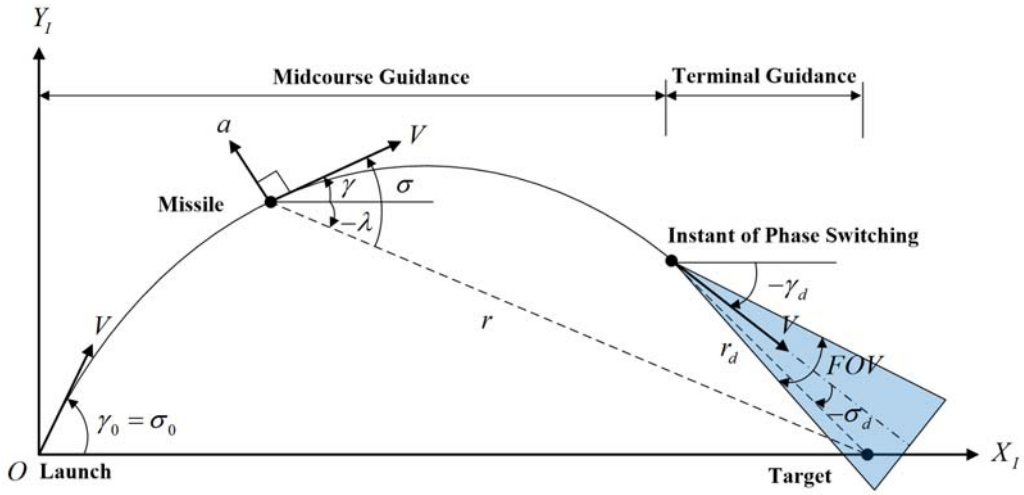

FIGURE 1. Engagement Geometry

quadratic optimal control theory. The terminal conditions for the midcourse phase are set as the desired values to lock on the target under seeker's physical constraints such as the FOV limit and the detection range. If the terminal conditions are chosen as the interception with impact angle constraint, the proposed midcourse guidance law can be used as the terminal guidance one.

3.1. **Midcourse Guidance Law.** Let us consider the following cost function weighted a power of range-to-go:

$$J = \frac{1}{2}\int_{r_0}^{r_d} \frac{a^2}{(r - r_d)^N} dr, \quad N \geq 0 \tag{3.1}$$

where N denotes a guidance gain. In case of $N = 0$, it is to solve a pure energy optimal guidance problem. Also, in case of $N > 0$, during the entire engagement, the control energy are distributed by the weight function of $(r - r_d)^{-N}$ in Eq. (3.1), so the huge guidance commands are generated at the initial phase and the acceleration becomes zero at the end of the guidance phase.

The Hamiltonian H of the guidance problem is

$$H = \frac{a^2}{2(r - r_d)^N} - \lambda_\sigma \left(\frac{a}{V^2} + \frac{\sigma}{r}\right) - \lambda_\gamma \frac{a}{V^2} \tag{3.2}$$

where λ_σ and λ_γ denote the co-states. Their differential equations with respect to r are given by

$$\frac{d\lambda_\sigma}{dr} = -\frac{\partial H}{\partial \sigma} = \lambda_\sigma \frac{1}{r} \tag{3.3}$$

$$\frac{d\lambda_\gamma}{dr} = -\frac{\partial H}{\partial \gamma} = 0 \tag{3.4}$$

where the terminal conditions of the co-states are $\lambda_{\sigma_d} = \nu_\sigma$ and $\lambda_{\gamma_d} = \nu_\gamma$. Integrating Eqs. (3.3) and (3.4) with the terminal conditions yields

$$\lambda_\sigma = v_\sigma \frac{r}{r_d} \tag{3.5}$$

$$\lambda_\gamma = v_\gamma \tag{3.6}$$

Using the optimality condition $\partial H/\partial r = 0$, we have the following optimal acceleration:

$$a = \frac{\nu_\sigma}{V^2 r_d} r \left(r - r_d\right)^N + \frac{\nu_\gamma}{V^2} \left(r - r_d\right)^N \tag{3.7}$$

Eq. (3.7) implies that the acceleration commands for $N = 0$ are linearly generated, and will not become zero at the end of the guidance phase because of the constant ν_γ. Also, $a\left(r_d\right) = 0$ when $N > 0$. The range-derivative of Eq. (3.7) is

$$\frac{da}{dr} = a' = \frac{\nu_\sigma}{V^2 r_d} \left[(1+N)\, r - r_d\right] \left(r - r_d\right)^{N-1} + \frac{\nu_\gamma}{V^2} N \left(r - r_d\right)^{N-1} \tag{3.8}$$

From Eq. (3.8), if $N \leq 1$, then $a'\left(r_d\right) \neq 0$. In addition, if $N > 1$, then $a'\left(r_d\right) = 0$.

Substituting Eq. (3.7) into Eq. (2.6) and then integrating these equations, we have

$$\begin{aligned} \sigma = &- \frac{\nu_\sigma}{V^4 r_d} \frac{1}{r} \left[\frac{\left(r - r_d\right)^{N+3}}{N+3} + 2 r_d \frac{\left(r - r_d\right)^{N+2}}{N+2} + r_d^2 \frac{\left(r - r_d\right)^{N+1}}{N+1} \right] \\ &- \frac{\nu_\gamma}{V^4} \left[\frac{\left(r - r_d\right)^{N+2}}{N+2} + r_d \frac{\left(r - r_d\right)^{N+1}}{N+1} \right] + \frac{C_\sigma}{r} \end{aligned} \tag{3.9}$$

$$\gamma = - \frac{\nu_\sigma}{V^4 r_d} \left[\frac{\left(r - r_d\right)^{N+2}}{N+2} + r_d \frac{\left(r - r_d\right)^{N+1}}{N+1} \right] - \frac{\nu_\gamma}{V^4} \frac{\left(r - r_d\right)^{N+1}}{N+1} + C_\gamma \tag{3.10}$$

where C_σ and C_γ are integration constants to be determined from the initial conditions. Therefore, using the initial conditions of Eq. (2.7), Eqs. (3.9) and (3.10) can be rewritten as

$$\sigma = \frac{\nu_\sigma}{V^4 r_d} \frac{1}{r} \left[G\left(r_0\right) - G\left(r\right)\right] + \frac{\nu_\gamma}{V^4} \left[H\left(r_0\right) - H\left(r\right)\right] + \sigma_0 \frac{r_0}{r} \tag{3.11}$$

$$\gamma = \frac{\nu_\sigma}{V^4 r_d} \left[P\left(r_0\right) - P\left(r\right)\right] + \frac{\nu_\gamma}{V^4} \left[Q\left(r_0\right) - Q\left(r\right)\right] + \gamma_0 \tag{3.12}$$

where

$$G(r) = \frac{(r-r_d)^{N+3}}{N+3} + 2r_d\frac{(r-r_d)^{N+2}}{N+2} + r_d^2\frac{(r-r_d)^{N+1}}{N+1} \tag{3.13}$$

$$H(r) = \frac{(r-r_d)^{N+2}}{N+2} + r_d\frac{(r-r_d)^{N+1}}{N+1} \tag{3.14}$$

$$P(r) = \frac{(r-r_d)^{N+2}}{N+2} + r_d\frac{(r-r_d)^{N+1}}{N+1} \tag{3.15}$$

$$Q(r) = \frac{(r-r_d)^{N+1}}{N+1} \tag{3.16}$$

Also, from the terminal conditions of Eq. (2.8), we have

$$\nu_\sigma = V^4 r_d \frac{[(\gamma_d-\gamma_0)H(r_0) - (\sigma_d r_d - \sigma_0 r_0)Q(r_0)]}{[P(r_0)H(r_0) - Q(r_0)G(r_0)]} \tag{3.17}$$

$$\nu_\gamma = -V^4 \frac{[(\gamma_d-\gamma_0)G(r_0) - (\sigma_d r_d - \sigma_0 r_0)P(r_0)]}{[P(r_0)H(r_0) - G(r_0)Q(r_0)]} \tag{3.18}$$

Substituting Eqs. (3.17) and (3.18) into Eq. (3.7), the open-loop optimal solution can be obtained as

$$\begin{aligned} a =& V^2 \frac{[(\gamma_d-\gamma_0)H(r_0) - (\sigma_d r_d - \sigma_0 r_0)Q(r_0)]}{[P(r_0)H(r_0) - Q(r_0)G(r_0)]} r(r-r_d)^N \\ & - V^2 \frac{[(\gamma_d-\gamma_0)G(r_0) - (\sigma_d r_d - \sigma_0 r_0)P(r_0)]}{[P(r_0)H(r_0) - G(r_0)Q(r_0)]} (r-r_d)^N \end{aligned} \tag{3.19}$$

If the initial states in Eq. (3.19) are taken as the current states, the closed-loop optimal solution is obtained as

$$a = -\frac{V^2}{(r-r_d)^2}\{(N+2)[(N+1)r + 2r_d](\gamma_d-\gamma) - (N+2)(N+3)(r_d\sigma_d - r\sigma)\} \tag{3.20}$$

The optimal midcourse guidance laws with various guidance gains N are shown in Table 1

TABLE 1. Examples of optimal terminal guidance laws with different N

N	Optimal Guidance Laws	Notes
0	$a = -\frac{V^2}{(r-r_d)^2}[2(r+2r_d)(\gamma_d-\gamma) - 6(r_d\sigma_d - r\sigma)]$	$a(r_d) \neq 0$
1	$a = -\frac{V^2}{(r-r_d)^2}[6(r+r_d)(\gamma_d-\gamma) - 12(r_d\sigma_d - r\sigma)]$	$a(r_d) = 0$
2	$a = -\frac{V^2}{(r-r_d)^2}[4(3r+2r_d)(\gamma_d-\gamma) - 20(r_d\sigma_d - r\sigma)]$	$a(r_d) = a'(r_d) = 0$

3.2. **Terminal Guidance Law.** The conditions to intercept a stationary target at the final time t_f are

$$\lim_{t \to t_f} r = 0 \tag{3.21}$$

$$\lim_{r \to 0} \sigma = 0 \tag{3.22}$$

By applying the interception conditions of Eqs. (3.21) and (3.22) to Eq. (3.20), we have

$$a = -\frac{V^2}{r} \left[(N+1)(N+2)(\gamma_d - \gamma) + (N+2)(N+3)\sigma \right] \tag{3.23}$$

Also, setting $\sigma = \gamma - \lambda$ and $r \approx V t_{go}$, where $t_{go} = t_f - t$, in Eq. (3.23), we have

$$a = -\frac{V}{t_{go}} \left[-(N+2)(N+3)\lambda + 2(N+2)\gamma + (N+1)(N+2)\gamma_f \right] \tag{3.24}$$

Equations (3.23) and (3.24) are optimal impact angle control guidance laws for homing guidance missiles against stationary targets. The optimal terminal guidance laws with various N are shown in Table 2.

TABLE 2. Examples of optimal terminal guidance laws with different N

N	Optimal Terminal Guidance Laws	Notes
0	$a = -\frac{V^2}{r} \left[2(\gamma_f - \gamma) + 6\sigma \right]$	$a(0) \neq 0$
1	$a = -\frac{V^2}{r} \left[6(\gamma_f - \gamma) + 12\sigma \right]$	$a(0) = 0$
2	$a = -\frac{V^2}{r} \left[12(\gamma_f - \gamma) + 20\sigma \right]$	$a(0) = a'(0) = 0$

Hence, from the results of Eqs. (3.23) and (3.24), it can be known that the proposed midcourse guidance law of Eq. (3.20) can be utilized as the terminal guidance one if $r_d = 0$ and $\sigma_d = 0$ for the final phase are chosen.

3.3. **Desired Look Angle and Relative Range Selection for the Midcourse Phase.** In the proposed midcourse guidance law, the desired look angle σ_d can be selected as an arbitrary value, but it should take into account the seeker's FOV limits to lock on the target during the midcourse phase. Let us define a look angle margin

$$\sigma_{\text{margin}} = FOV/2 - |\sigma(r_d)| \tag{3.25}$$

From Eq. (3.25), to maximize the look angle margin σ_{margin}, the desired look angle σ_d should be set to zero. Although, in aerodynamically controlled missiles, the seeker's FOV is defined as an angle between the missile body axis and the LOS (i.e., the sum of the lead angle, defined in the velocity axis and the LOS, and the AOA), the AOA becomes zero at the instant of the handover due to zero acceleration when using the proposed midcourse guidance law with $N > 0$. This means that the seeker's FOV is identical to the look angle defined in previous section. In the vertical plane engagement affected by the gravity, the gravity compensation term $g \cos(\gamma)$ should be added to the guidance command, so the acceleration at the instant of

the handover will not become zero. However, the AOA generated by the gravity is small, i.e., $|a(r_d)| \leq g$ for $N > 0$, so we can use the look angle, defined previously, for controlling the seeker's FOV limit.

The desired relative range r_d is set to the seeker's detection range because the navigation errors are increased as the midcourse phase takes long, which require more control energy to correct the terminal guidance errors. Hence, the desired look angle and relative range are chosen as

$$\sigma_d = 0 \tag{3.26}$$

$$r_d = r_{\text{seeker}} \tag{3.27}$$

4. Numerical Examples

In this section, nonlinear simulations are performed to investigate the performance of the proposed guidance laws. First, for the entire engagement, using both of the proposed midcourse and terminal guidance laws, and using the only terminal one are compared in order to check the importance of the midcourse phase for a missile with a narrow FOV of the seeker. Second, nonlinear simulations are performed to confirm the characteristics of the proposed guidance laws when various guidance gains and impact angles are given. Finally, the performance of the proposed guidance law is described for a realistic missile system having an autopilot lag and acceleration limit.

4.1. **Comparison Study.** Nonlinear simulations are performed to investigate the importance of the midcourse phase for a missile with a limited FOV of the seeker. The initial conditions for nonlinear simulations are shown in Table 3, and the guidance gain is chosen as $N = 0$, which generates pure energy minimization control inputs.

The missile trajectories, lateral acceleration, look angles, and flight path angles are shown in Figs. 2-5, where the legends MID+TER and TER denote the implementation of both the proposed midcourse and terminal guidance laws, and the only terminal one, respectively.

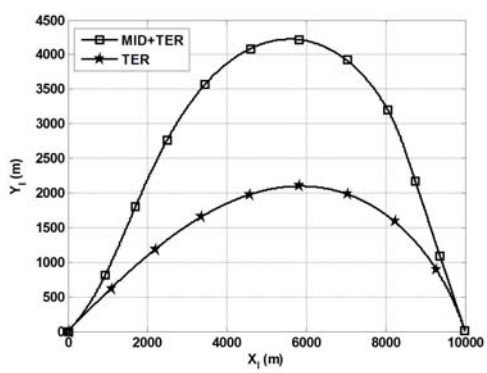

FIGURE 2. Missile Trajectories for Comparison Study

As shown in Fig. 2, the missile trajectories using both the proposed laws are more highly curved because the missile enters the impact angle plane at shorter relative range than using the only terminal one.

There is no uncertainty and noise in these simulations, so, in case of MID+TER, the missile is guided on the collision course, which intercepts the target without any control effort, after the handover. The acceleration profiles are shown in Fig. 3, they are nearly not generated during the terminal phase in case of MID+TER because of the collision course.

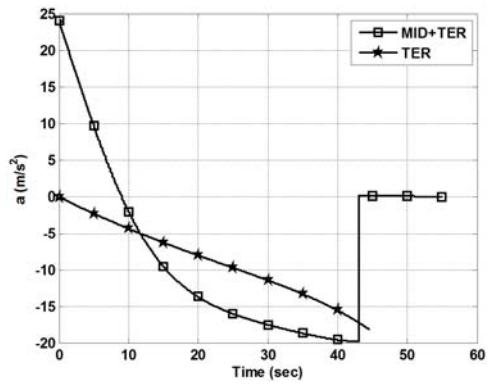

FIGURE 3. Lateral Acceleration for Comparison Study

However, when using the only terminal guidance law during the entire engagement, the acceleration is almost linearly generated. As shown Fig. 4, the look angle at the detection range of $r_d = 3$ km becomes zero for the case of MID+TER. However, in case of TER, the look angle becomes 19.6 deg, so it is impossible to lock on the target and then may result in mission failure.

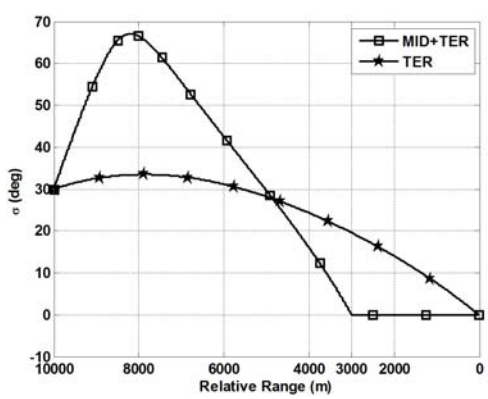

FIGURE 4. Look Angles for Comparison Study

Figure 5 presents the flight path angles, and the desired impact angles are achieved for both cases. From these results, to implement the impact angle control for a missile with the seeker's FOV limit, the midcourse trajectory will be well designed to lock on the target when the target is located in the place where the seeker cannot detect it from the initial missile position.

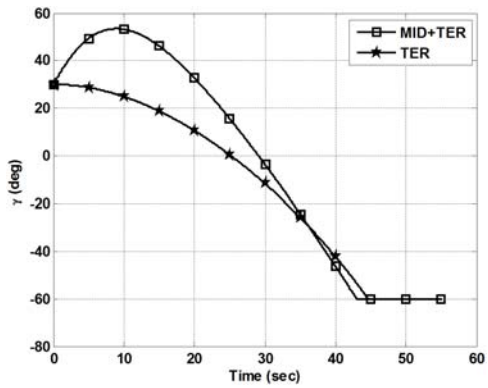

FIGURE 5. Flight Path Angles for Comparison Study

TABLE 3. Initial Conditions for Nonlinear Simulations

Parameters	Values
Missile Position, (x_0, y_0)	$(0, 0)$ km
Target Position, (x_f, y_f)	$(10, 0)$ km
Missile Speed, V	250 m/s
Launch Angle, $\gamma_0 = \sigma_0$	30 deg
Seeker's FOV	± 15 deg (or 30 deg)
Seeker's Detection Range, $r_{\text{seeker}} = r_d$	3 km
Impact Angle, $\gamma_d = \gamma_f$	-90 deg ~0 deg

4.2. **Characteristics of an Optimal Guidance Law.** To investigate basic properties of the proposed guidance law, nonlinear simulations for various guidance gains, when the impact angle is fixed, are performed. In addition, nonlinear simulations for various impact angles, when the guidance gain is fixed, are carried out. The simulations are terminated at the instant of the seeker's lock-on because the missile flights on the collision course after the handover, which will form the same flight path during the terminal phase.

4.2.1. *Case 1: Various Guidance Gains N.* The simulation results for the case of various guidance gains are shown in Figs. 6-9 and Table 4. As shown in Fig. 6, higher guidance gains are chosen, more the missile trajectories are highly curved.

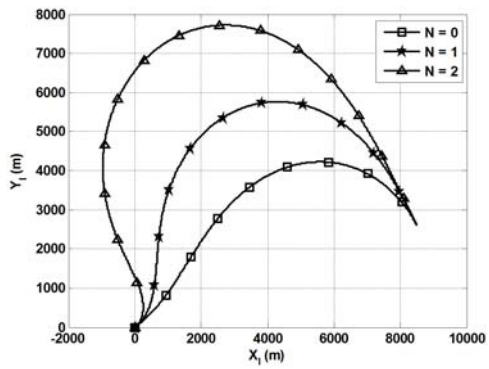

FIGURE 6. Missile Trajectories for Various Guidance Gains

From Fig. 7, by the weighting function, the largest guidance commands are generated for $N = 2$, and the acceleration becomes zero at the end of the midcourse phase except for $N = 0$.

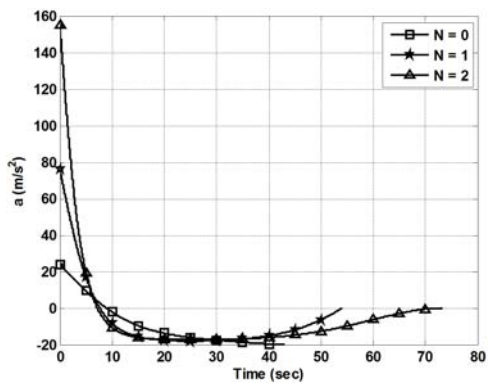

FIGURE 7. Lateral Acceleration for Various Guidance Gains

As shown in Fig. 8, in all cases, the look angles converge on zero, so the seeker could lock on the target at the detection range. However, in case of $N = 0$, since the AOA is not zero at the detection range due to non-zero acceleration, the look angle in a realistic missile system could not become zero. Hence, the proposed midcourse guidance law with $N > 0$ is more practical to ensure the maximum look angle margin. Figure 9 shows that the desired impact angle constraints are satisfied for all cases.

From the control energy result shown in Table 4, the smallest energy is consumed in $N = 0$, which generates a pure energy minimization control inputs, and the largest energy is required

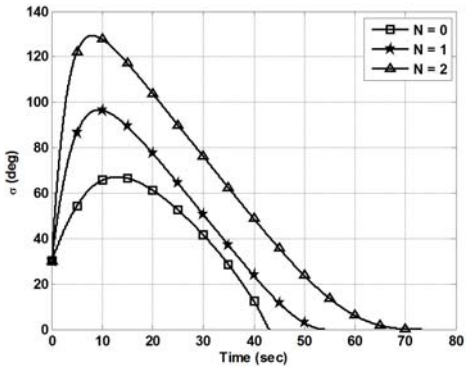

FIGURE 8. Look Angles for Various Guidance Gains.

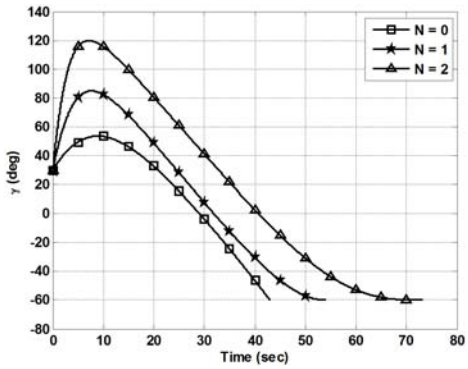

FIGURE 9. Flight Path Angles for Various Guidance Gains.

in $N = 2$. Therefore, to perform next nonlinear simulations for various impact angles, we choose $N = 1$ as a proper guidance gain, which satisfies zero acceleration at the detection range and does not generate large guidance commands.

TABLE 4. Comparison of Control Energy

	OGL with $N = 0$	OGL with $N = 1$	OGL with $N = 2$
$J = \frac{1}{2}\int_t^{t_f} a^2 dt,\ \mathrm{m}^2/s^3$	4852.9	10525.4	23762.4

4.2.2. *Case 2: Various Impact Angles.* Nonlinear simulations for γ_d =0 deg, -30 deg, -60 deg, and -90 deg are performed, and their results are presented in Figs. 10-13. From Fig. 10, as high impact angles are chosen, the missile trajectories are highly shaped.

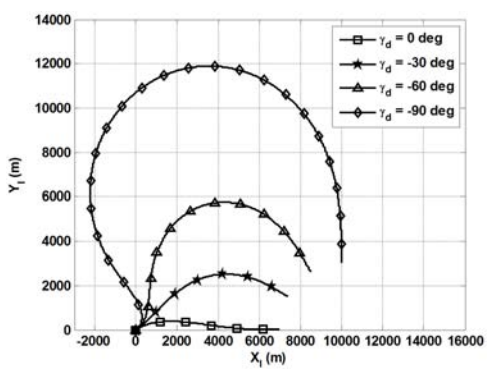

FIGURE 10. Missile Trajectories for Various Impact Angles

As shown in Fig. 11, the largest guidance commands are generated in the beginning of the engagement, and the acceleration becomes zero at the end of the midcourse phase in all cases. As shown in Fig. 12, the look angles converge on zero near the final time.

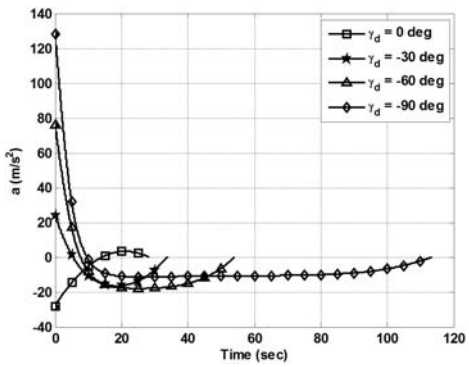

FIGURE 11. Lateral Acceleration for Various Impact Angles

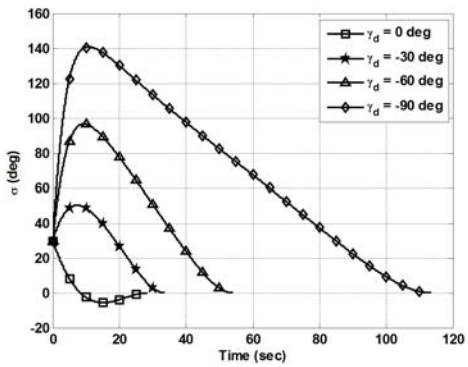

FIGURE 12. Look Angles for Various Impact Angles

Also, Fig. 13 presents that the flight path angles satisfy the desired impact angles, respectively.

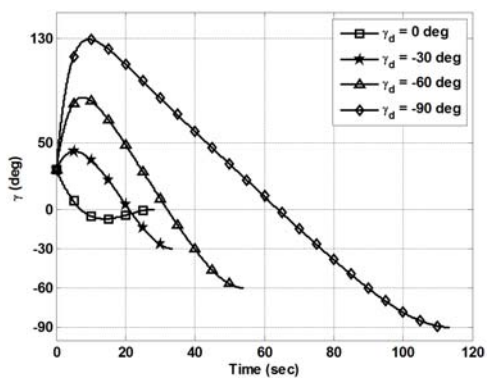

FIGURE 13. Flight Path Angles for Various Impact Angles

4.3. **First-Order Autopilot Lag with Acceleration Limit.** A realistic missile system has an autopilot lag and acceleration limit, which causes the terminal miss-distance and impact angle errors. Therefore, through nonlinear simulations, the robustness of the proposed guidance law is checked with respect to these nonlinearities. The autopilot system is modeled as the following first-order one:

$$\frac{a}{a_c} = \frac{1}{s\tau + 1} \tag{4.1}$$

where a_c is the control input and τ is the first-order time constant. We choose the first-order time constant as $\tau = 0.3$ s and the maximum acceleration limit as $|a_c| \leq 50$ m/s^2. Also, impact angles are set to γ_d =-45 deg, -60 deg, and -75 deg, and the guidance gain is set to $N = 1$. Since the guidance commands for the midcourse phase can generate infinite values near the desired relative range due to the system lag and uncertainty in the real engagement environment of the missile, the relative range is used as a fixed value when $r < (r_d + 30)$ m and then terminal guidance commands are calculated using the current relative range after the handover.

Nonlinear simulation results with the first-order autopilot lag are presented in Figs. 14-17. Figures 14 and 15 show the interception trajectories and missile acceleration, respectively.

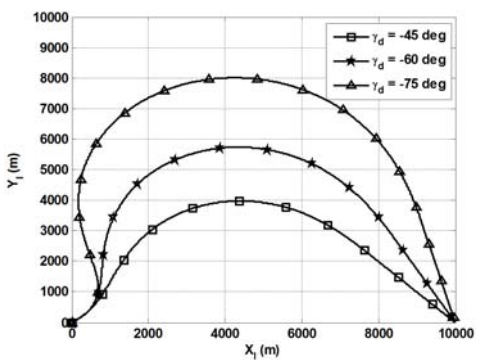

FIGURE 14. Missile Trajectories for First-Order Autopilot Lag

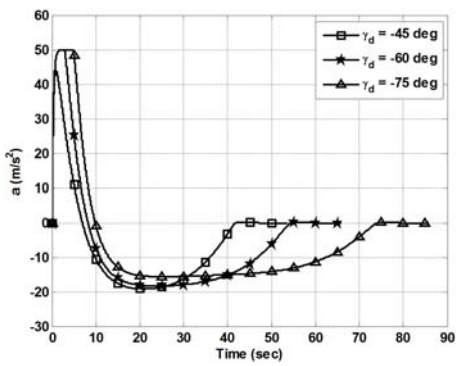

FIGURE 15. Lateral Acceleration for First-Order Autopilot Lag

Also, Figs. 16 and 17 present the look angles and the flight path angles, respectively. From these figures, it can be known that the proposed laws successfully impact the target with the desired terminal angle after locking on the target under the realistic missile environment.

5. CONCLUSIONS

This paper has presented an optimal guidance law with impact angle constraint considering the seeker's lock-on condition. The proposed guidance law can be utilized in both of the midcourse and terminal phases by changing the desired look angle and relative range values to the final interception conditions. During the midcourse phase, to maximize the look angle margin and homing time, the desired look angle and relative range are set to zero and the detection range of the seeker, respectively. The performance of the proposed guidance law is investigated via nonlinear simulations for various engagement conditions.

REFERENCES

[1] M. Kim and K. V. Grider, Terminal Guidance for Impact Attitude Angle Constrained Flight Trajectories, IEEE Transactions on Aerospace and Electronic Systems, **9**(6) (1973), 852–859.

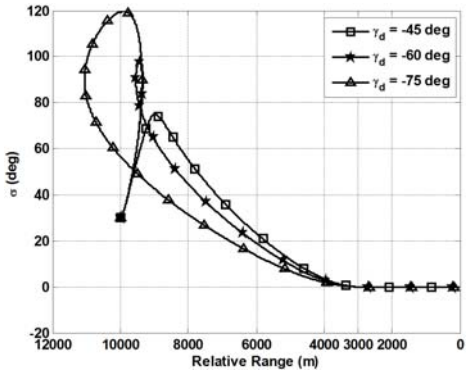

FIGURE 16. Look Angles for First-Order Autopilot Lag

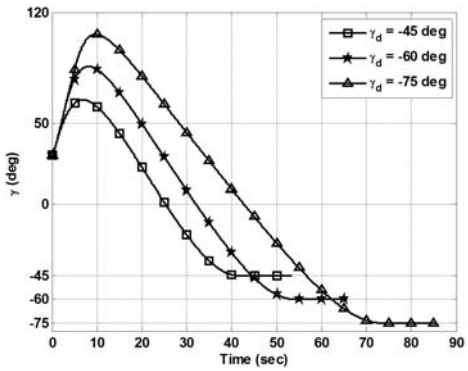

FIGURE 17. Flight Path Angles for First-Order Autopilot Lag

[2] A. E. Bryson Jr. and Y.-C. Ho, Applied Optimal Control, New York: Wiley, 1975.
[3] T. L. Song, S. J. Shin, and H. Cho, Impact Angle Control for Planar Engagements, IEEE Transactions on Aerospace and Electronic Systems, **35**(4) (1999), 1439–1444.
[4] C. K. Ryoo, H. Cho, and M. J. Tahk, Optimal Guidance Laws with Terminal Impact Angle Constraint, Journal of Guidance, Control, and Dynamics, **28**(4) (2005), 724–732.
[5] C. K. Ryoo, H. Cho, and M. J. Tahk, Time-to-Go Weighted Optimal Guidance with Impact Angle Constraints, IEEE Transactions on Control Systems Technology, **14**(3) (2006), 483–492.
[6] A. Ratnoo and D. Ghose, State-Dependent Riccati-Equation-Based Guidance Law for Impact-Angle-Constrained Trajectories, Journal of Guidance, Control, and Dynamics, **32**(1) (2009), 320–325.
[7] Y. I. Lee, S. H. Kim, and M. J. Tahk, Optimality of Linear Time-Varying Guidance for Impact Angle Control, IEEE Transactions on Aerospace and Electronic Systems, **48**(3) (2012), 2802–2817.
[8] B. S. Kim, J. G. Lee, and H. S. Han, Biased PNG law for Impact with Angular Constraint, IEEE Transactions on Aerospace and Electric Systems, **34**(1) (1998), 277–288.
[9] I. R. Manchester and A. V. Savkin, Circular-Navigation-Guidance Law for Precision Missile/Target Engagements, Journal of Guidance, Control and Dynamics, **29**(2) (2006), 314–320.
[10] A. Ratnoo and D. Ghose, Impact Angle Constrained Interception of Stationary Targets, Journal of Guidance, Control, and Dynamics, **31**(6) (2008), 1816–1821.
[11] A. Ratnoo and D. Ghose, Impact Angle Constrained Guidance Against Nonstationary Nonmaneuvering Targets, Journal of Guidance, Control, and Dynamics, **32**(1) (2010), 269–275.
[12] K. S. Erer and O. Merttop?uo?lu, Indirect Impact-Angle-Control Against Stationary Targets Using Biased Pure Proportional Navigation, Journal of Guidance, Control, and Dynamics, **35**(2) (2012), 700–703.
[13] I. H. Whang, Target Pointing Guidance using Optimal Control, (in Korean), The Transactions of The Korean Institute of Electrical Engineers, **48A**(7) (1999), 881–888.
[14] I. S. Jeon and J. I Lee, Guidance Law to Reach Circular Target Area With Grazing Angle Constraint, (in Korean), Journal of The Society for Aeronautical and Space Sciences, **36**(9) (2008), 884–890.